

RESEARCH

Open Access



# A deep learning model for radiological measurement of adolescent idiopathic scoliosis using biplanar radiographs

Kunjie Xie<sup>1</sup>, Suping Zhu<sup>2</sup>, Jincong Lin<sup>1</sup>, Yi Li<sup>2</sup>, Jinghui Huang<sup>1</sup>, Wei Lei<sup>1\*</sup> and Yabo Yan<sup>1\*</sup>

## Abstract

**Background** Accurate measurement of the spinal alignment parameters is crucial for diagnosing and evaluating adolescent idiopathic scoliosis (AIS). Manual measurement is subjective and time-consuming. The recently developed artificial intelligence models mainly focused on measuring the coronal Cobb angle (CA) and ignored the evaluation of the sagittal plane. We developed a deep-learning model that could automatically measure spinal alignment parameters in biplanar radiographs.

**Methods** In this study, our model adopted ResNet34 as the backbone network, mainly consisting of keypoint detection and CA measurement. A total of 600 biplane radiographs were collected from our hospital and randomly divided into train and test sets in a 3:1 ratio. Two senior spinal surgeons independently manually measured and analyzed spinal alignment and recorded the time taken. The reliabilities of automatic measurement were evaluated by comparing them with the gold standard, using mean absolute difference (MAD), intraclass correlation coefficient (ICC), simple linear regression, and Bland-Altman plots. The diagnosis performance of the model was evaluated through the receiver operating characteristic (ROC) curve and area under the curve (AUC). Severity classification and sagittal abnormalities classification were visualized using a confusion matrix.

**Results** Our AI model achieved the MAD of coronal and sagittal angle errors was 2.15° and 2.72°, and ICC was 0.985, 0.927. The simple linear regression showed a strong correlation between all parameters and the gold standard ( $p < 0.001$ ,  $r^2 \geq 0.686$ ), the Bland-Altman plots showed that the mean difference of the model was within 2° and the automatic measurement time was 9.1 s. Our model demonstrated excellent diagnostic performance, with an accuracy of 97.2%, a sensitivity of 96.8%, a specificity of 97.6%, and an AUC of 0.972 (0.940–1.000). For severity classification, the overall accuracy was 94.5%. All accuracy of sagittal abnormalities classification was greater than 91.8%.

**Conclusions** This deep learning model can accurately and automatically measure spinal alignment parameters with reliable results, significantly reducing diagnostic time, and might provide the potential to assist clinicians.

**Keywords** Adolescent idiopathic scoliosis, Deep learning, Cobb angle, Sagittal alignment parameter, Biplanar radiographs

\*Correspondence:

Wei Lei

leiwei@fmmu.edu.cn

Yabo Yan

yanyabo@fmmu.edu.cn

Full list of author information is available at the end of the article



© The Author(s) 2025. **Open Access** This article is licensed under a Creative Commons Attribution-NonCommercial-NoDerivatives 4.0 International License, which permits any non-commercial use, sharing, distribution and reproduction in any medium or format, as long as you give appropriate credit to the original author(s) and the source, provide a link to the Creative Commons licence, and indicate if you modified the licensed material. You do not have permission under this licence to share adapted material derived from this article or parts of it. The images or other third party material in this article are included in the article's Creative Commons licence, unless indicated otherwise in a credit line to the material. If material is not included in the article's Creative Commons licence and your intended use is not permitted by statutory regulation or exceeds the permitted use, you will need to obtain permission directly from the copyright holder. To view a copy of this licence, visit <http://creativecommons.org/licenses/by-nc-nd/4.0/>.

## Introduction

Adolescent Idiopathic Scoliosis (AIS) is a common three-dimensional spinal deformity with an unclear etiology, which may be related to factors such as estrogen, low bone density, and genetic predisposition [1–3]. The prevalence of AIS is about 1–3%, with a higher incidence in girls than boys [1]. Without prompt intervention, deformity may worsen and reduce the quality of life. School screening is one of the important methods for early detection of AIS [4], and following a positive screening result, further imaging with anteroposterior (AP) and lateral (LAT) X-rays is usually necessary [3].

Accurate assessment of spinal alignment is crucial for making proper treatment. It is based on radiographic measurements from the biplanar radiographs, including the coronal Cobb angle (CA) and sagittal CA such as the proximal thoracic kyphosis (PTK), mid-thoracic kyphosis (MTK), and thoracolumbar sagittal alignment (TSA). On AP X-rays, the diagnostic gold standard for AIS is a coronal CA exceeding 10°, and AIS is typically classified into normal ( $CA < 10^\circ$ ), mild ( $10^\circ$ – $25^\circ$ ), moderate ( $25^\circ$ – $45^\circ$ ), and severe ( $> 45^\circ$ ). Clinicians select treatment strategies based on the severity, including regular monitoring, brace, and surgical correction [1, 5]. For LAT X-rays, the measurement of the sagittal CA is used to assess the sagittal plane balance of the spine, which is crucial for surgical planning. However, the diagnosis and evaluation of AIS rely mainly on manual measurements by clinicians, which are time-consuming, labor-intensive, and subjective, leading to considerable measurement errors [6, 7]. Thus, accurately and rapidly measuring and analyzing AIS parameters remains a challenge.

In recent years, artificial intelligence (AI), particularly deep learning, has emerged as a promising tool for image processing and is gradually being applied in the field of scoliosis [8–11]. AI-based algorithms can automatically detect key points and segment vertebrae from spinal images, enabling the automatic measurement of radiological parameters. This can significantly streamline clinical workflows and enhance diagnostic efficiency. However, current research mainly focuses on the automatic measurement of the coronal plane [8–11], with limited studies on the automatic measurement of the sagittal plane [12]. Furthermore, there is a lack of comprehensive diagnostic and assessment research based on biplanar radiographs, which restricts the application of AI in treatment planning and follow-up assessments.

Therefore, this study aims to develop and validate a deep learning-based model that can automatically, accurately, and rapidly measure parameters from biplanar

X-rays, and perform diagnosis and assessment of AIS, thereby assisting clinicians in AIS practice.

## Materials and methods

### Patients

This study was approved by the Ethical Review Board of the Xijing Hospital of the Air Force Military Medical University. As this study was retrospective, the ethics committee waived the requirement for informed consent. All radiographs were taken by a digital X-ray machine (Definium 6000 DR, General Electric Company, United States). When taking an AP radiograph, the patient should stand naturally, barefoot, with feet shoulder-width apart. The knees should be naturally extended, arms should hang loosely by the sides. If the leg length discrepancy is greater than 2 cm, the shorter side should be elevated to keep the pelvis level. For the LAT radiograph, the patient should stand in the same manner, with arms bent at the elbows at a 90° and raised horizontally in front of the chest. All radiographic examinations are used for clinical measurement to diagnose or monitor scoliosis progression.

Inclusion criteria: (1) Includes complete biplane X-ray images; (2) Suspected or diagnosed as AIS; (3) 10–18 years old; (4) The interval between two examinations for the same patient exceeds 6 months; (5) no significant rotation or tilt for radiographs.

Exclusion criteria: (1) Poor image quality; (2) Severe pelvic tilt; (3) Previous history of spinal surgery; (4) Congenital vertebral abnormalities or other musculoskeletal disorders; (5) Wearing braces.

Based on the inclusion and exclusion criteria mentioned above, we collected a total of 600 AP and LAT full spinal radiographs taken in the radiology department from October 2021 to July 2023. A dataset was constructed, including 276 males and 324 females with a mean age of  $15.3 \pm 6.1$  years. The dataset consists of radiographic images of normal individuals and patients with scoliosis. We used the random number table method to divide the dataset into train and test sets in a ratio of 3:1. The demographic information of the dataset was presented in Table 1.

### Definition of parameters and classification of severity

For coronal parameters, CA is defined as the angle between the upper endplate of the upper end vertebra (UEV) and the lower endplate of the lower end vertebra (LEV) [1, 6, 13], and end vertebra (EV) refers to the most inclined vertebra in the spine. According to the clinical diagnostic standard, a CA greater than 10° can diagnose scoliosis [1]. For the severity classification of deformity, if the coronal Cobb angle is 0–10°, it

**Table 1** Demographics in data set

Parameter	Train set	Test set
No. of patients	454	146
Female: male	229:225	95:51
Age in years(95%CI)	14.2(13.6–14.8)	12.9(11.8–14.0)
<i>Diagnosis</i>		
No scoliosis	224	84
Scoliosis	230	62
<i>Classification of severity</i>		
Normal( $CA \leq 10^\circ$ )	224	84
Mild( $10^\circ < CA \leq 25^\circ$ )	111	22
Moderate ( $25^\circ < CA \leq 45^\circ$ )	77	23
Severe( $> 45^\circ$ )	42	17

95%CI: 95% confidence interval

is considered normal; 10–25° is classified as mild, 25–45° as moderate, and greater than 45° as severe. For sagittal parameters, we calculated PTK, MTK, and TSA, which are widely used in Lenke classification [14]. The previously reported normal range of PTK, MTK, and TSA were 0–20° [14], 10–40° [14, 15], and 0–10 [16], respectively.

**Model construction**

**Image annotation**

Two junior orthopedics doctors used the image annotation software "Labelme" to manually label T1-L5 in the AP and LAT radiographs. Specifically,454 X-ray images in the train set are randomly assigned to those two

doctors for annotation. Before independent annotation, both of them had undergone rigorous training on the standardization of scoliosis radiographic diagnosis and annotation software usage, unifying the definition and methods of annotation. We invited two senior spinal surgeons to review the annotated images one by one. Any inaccurate annotations will be corrected. Finally, the annotated images were saved in JSON format.

**Network structure**

For the input spinal AP and LAT images, we adjusted the image size by uniformly resizing all images to 1024×512. Subsequently, image grayscale, denoising, normalization, and other processing were carried out to obtain higher-quality images while reducing subsequent computational complexity; Finally, to enhance the model’s generalization ability and adaptability to variations in imaging data. data augmentation techniques including random flipping, translation, and scaling are employed.

In this study, we adopted ResNet34 [17] as the basic framework and improved it by integrating the network characteristics of U-net (Fig. 1). This design effectively solves the common problem of gradient vanishing in deep network training, while utilizing ResNet34’s deep residual learning mechanism to endow the network with powerful feature extraction capabilities. In addition, skip connections enable the network to integrate deep high-level semantic features and shallow detail features at different levels, thereby simultaneously utilizing global contextual information and local fine information in image analysis [18, 19]. This combination not only

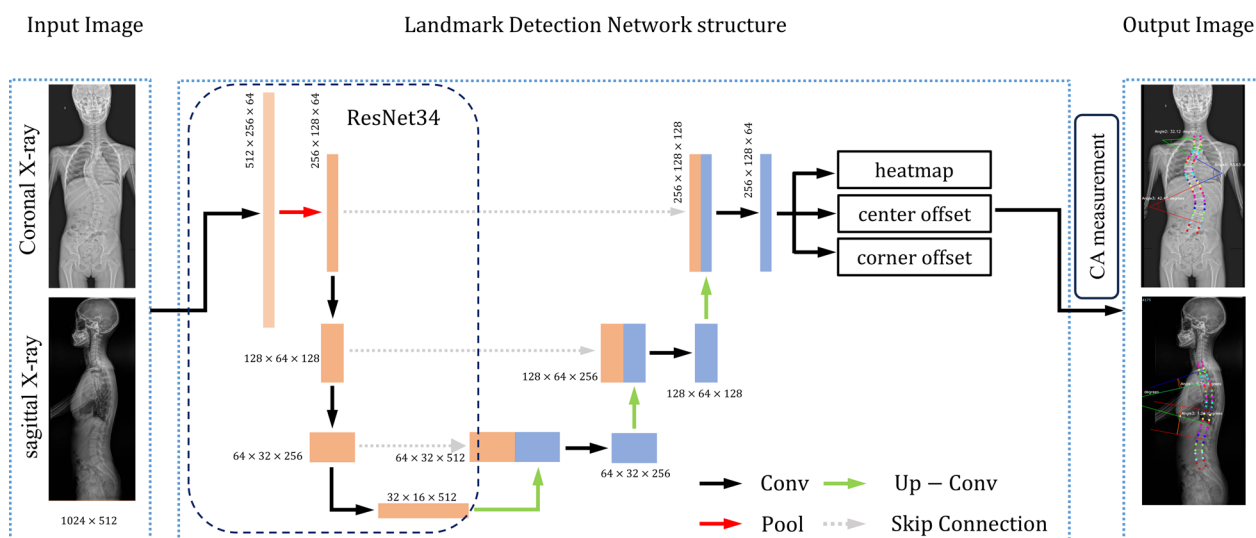


**Fig. 1** Model structure and diagnostic process. After inputting the coronal and sagittal X-rays of the full spine, our model will automatically perform landmark detection and CA measurement, output diagnostic results, and then evaluate the severity of scoliosis and sagittal plane abnormalities based on the range of parameter values. CA: Cobb angle

improves the network’s understanding of image content but also enhances its localization accuracy in complex medical image processing tasks. The residual network performs multiple convolutions and pooling operations on the image to extract high-level semantic feature maps at different levels of the image. Then, skip connections are used to combine deep and shallow features. We constructed a heatmap, center offset, and corner offset in the output layer [19].

The heatmap is used to locate the center of the vertebra and can be represented by a Gaussian disk, whose calculation method is the same as Yi et al. [19]. The center offset is used to map the reduced feature map after extracting the center point back to the original image, while the corner offset is the vector pointing from the center of the vertebra to the vertebral corner, used to locate the four vertebra corners. In this deep learning training process, the supervision module includes heatmap loss, center offset loss, and corner offset loss. Finally, our model identified the top left, top right, bottom left, and bottom right corners of each vertebral body based on the coordinates obtained from vertebra corner detection (Fig. 1).

**CA measurement**

On the AP radiograph, the coordinates of the upper left, upper right, lower right, and lower left corners of the vertebra in the plane rectangular coordinate system are denoted as  $A(x_1, y_1)$ ,  $B(x_2, y_2)$ ,  $C(x_3, y_3)$ , and  $D(x_4, y_4)$  respectively. Based on the detected four vertebral corners, identify the midpoint coordinates  $P(x_1 + x_3/2, y_1 + y_3/2)$  and  $Q(x_2 + x_4/2, y_2 + y_4/2)$  on the left and right sides of each vertebra. The straight line connecting the two represents the inclination of the vertebra and is denoted as  $\vec{PQ}$ . Thus, a total of 17 vectors, from T1 to L5, are obtained, The angle  $\theta$  between any two lines  $i$  and  $j$  can be calculated using the following formula:

$$\theta = \cos^{-1} \frac{\vec{P_j Q_j} \cdot \vec{P_k Q_k}}{|\vec{P_j Q_j}| |\vec{P_k Q_k}|}$$

Consistent with Sun et al. [11], our model first determines the CA of the major curve in a recursive manner, and then detects compensatory curves based on the type of scoliosis. Specifically, if the major curve is a thoracic curve, the model automatically continues to detect compensatory curves above and below the major curve in a recursive Method and calculates their CAs. Similarly, if the major curve is a thoracolumbar/lumbar curve, the model automatically detects the compensatory curve above the major curve. For the sagittal curve, our model initially locates the vertebral sequence from T1

to L5, and then automatically detects the four corners of each vertebra. Based on this, our model calculates the PTK, MTK, and TSA respectively.

**Manual measurement**

Two spinal surgeons measured alignment parameters through MicroDicom viewer (MicroDicom Ltd., Sofia, Bulgaria), then diagnosed and classified the severity of all radiographs in the test set, and recorded the time taken. The test set radiographs were divided into a normal group (84 cases, Cobb angle range 0–10°) and a patient group (62 cases, Cobb angle range 10–77.7°). The CA in the normal group was relatively small, even some curves were difficult to distinguish. Therefore, we only measured the CA of the major and minor curves in the patient group, while the sagittal CAs of both groups were measured. A retest was conducted to evaluate the reliability of the intro-observer and inter-observer after a four-week interval. The average of all measurements was used as the gold standard (GS) for this study. We tested the inter-observer consistency of parameter measurement between two experts and found a MAD of 1–4°(mean 2.5°±1.6°)and the agreements were excellent with an ICC of 0.969.

**Statistical analysis**

The evaluation of the model was based on the test set. For parameters measurement, the reliability of the model was calculated through the ICC and its 95% confidence interval, where ICC < 0.50, 0.50–0.75, 0.75–0.90, and > 0.90 are considered poor, moderate, good, and excellent, respectively [20]. The validity of the model was evaluated through Simple Linear Regression and Bland-Atman plots. The ROC curve and AUC were used to evaluate the diagnostic performance of the model. The accuracy, sensitivity, and specificity of the model classification were calculated using a confusion matrix. Use paired sample t-test to compare the time difference between the model and expert diagnosis.

The above data processing and statistical analysis were conducted using GraphPad Prism (Version 9.5.1, GraphPad; San Diego, United States) software.  $P < 0.05$  indicates statistical significance.

**Results**

**Comparison of model predictive results with the gold standard**

To evaluate the accuracy of the model in measuring coronal CA, we calculated the MAD between the model and the GS (Table 2). The MAD(± SD) of the PT, MT, and TL/L were 1.87° (± 1.43°), 2.23° (± 1.80°), and 2.33° (± 1.76°), respectively. Additionally, We tested the consistency of the model in automatically identifying

**Table 2** Inter-rater reliability of the Cobb angle measurements and end vertebra: Gold standard vs AI

Parameter	MAD	SD	ICC(95%CI)
<i>Coronal</i>			
Proximal thoracic CA	1.87°	1.43°	0.972(0.953–0.983)
Main thoracic CA	2.23°	1.80°	0.987(0.978–0.992)
Thoracolumbar/lumbar CA	2.33°	1.76°	0.979(0.965–0.985)
Total CA	2.15°	1.69°	0.985(0.979–0.989)
UEV	0.57	0.99	0.967(0.949–0.978)
LEV	0.53	0.71	0.982(0.973–0.989)
<i>Sagittal</i>			
Proximal thoracic kyphosis	2.86	2.00	0.828(0.769–0.873)
Mid-thoracic kyphosis	3.20	2.05	0.931(0.905–0.949)
Thoracolumbar sagittal alignment	2.11	1.75	0.875(0.931–0.908)
Total CA	2.72	1.99	0.927(0.912–0.939)

MAD: mean absolute difference; SD: standard difference; ICC:intra-class correlation coefficient; CA: Cobb angle

the end vertebrae and found that, compared to the gold standard, the mean errors in identifying the UEV and LEV were approximately 0.57 and 0.53 vertebrae, respectively. The consistency was nearly perfect. For the sagittal alignment parameters, PTK, MTK, and

TSA, they were 2.00 °(±2.00°), 3.20° (±2.05°), and 2.11° (±1.75°), respectively. Overall, coronal prediction is more accurate than sagittal prediction, with a smaller MAD(2.15 ° ± 1.69°). The ICC of all parameters between AI and GS was between 0.985 and 0.927 coronally and sagittally, and Table 2 shows that its reliability performance in coronal TL/L and sagittal MTK is more satisfactory. Overall, the reliability of coronal measurements is higher.

Simple linear regression showed a strong correlation between the model and the GS( $r^2 \geq 0.686$ ,  $p < 0.001$ , Fig. 2). The slopes measured in the coronal and sagittal parameters were 0.992 and 0.907, respectively, both close to the perfect line, indicating that the measured values are completely consistent with the GS. The Bland–Altman plots showed the differences between the model and the GS (Fig. 3), where the 95% limits of agreement(95%LoA) for PT, MT, and TL/L were  $-4.484^\circ - 4.774^\circ$  (Bias =  $-0.1450^\circ$ ),  $-5.120^\circ - 5.913^\circ$  (Bias =  $-0.3967^\circ$ ), and  $-4.538^\circ - 6.312^\circ$  (Bias =  $0.8871^\circ$ ), respectively. The 95% LoA for total CA was  $-4.736^\circ - 5.697^\circ$  (Bias =  $0.4803^\circ$ ). The 95% LoA for PTK, MTK, and TSA were  $-4.851^\circ - 7.693^\circ$  (Bias =  $1.421^\circ$ ),  $-4.610^\circ - 8.385^\circ$  (Bias =  $-0.3967^\circ$ ), and  $-4.975^\circ - 5.761^\circ$  (Bias =  $0.0363^\circ$ ), respectively. The 95% LoA for sagittal CA is  $-4.947^\circ - 7.395^\circ$  (Bias =  $1.224^\circ$ ).

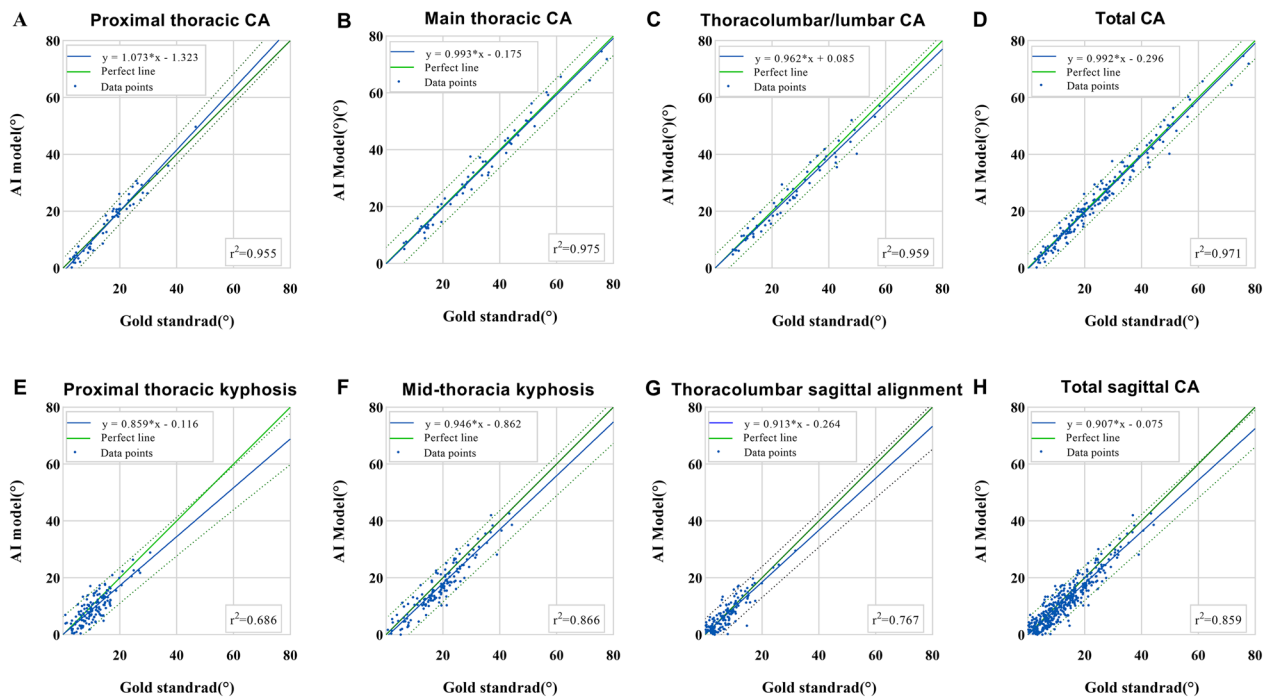


**Fig. 2** Linear regression analysis for the coronal and sagittal parameters. **A–D** showed the regression results of the coronal parameters, including PT, MT, TL/L and total CAs. **E–H** showed the regression results of the sagittal parameters, including PTK, MTK, TSA, and total sagittal CAs

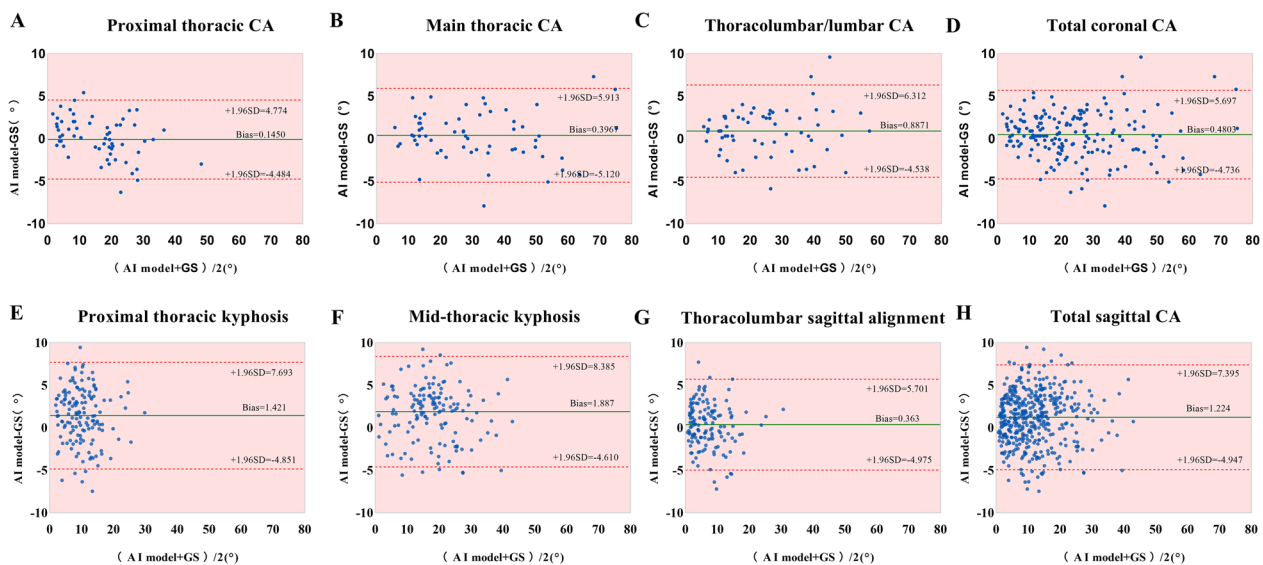


**Fig. 3** Comparison of automatic and manual measurement. **A–D** showed the Bland-Altman plot of the coronal parameters, including PT, MT, TL/L, and total CAs. **E–H** showed the Bland-Altman plot of the sagittal parameters, including PTK, MTK, TSA, and total sagittal CAs. All the Bland-Altman plots showed perfect agreements between the model and GS

### Performance of diagnosis and classification of model

The ROC curve demonstrates the performance of AI in diagnosing scoliosis (Fig. 4), AUC is 0.972 (0.940–1.000), with an accuracy of 97.2% (142/146), sensitivity of 96.8% (60/62), and specificity of 97.6% (82/84). Among the 84 images diagnosed as "normal" by experts, 2 were diagnosed as "patients" by the model. The confusion matrix shows the results of the model in severity classification and sagittal alignment evaluation (Fig. 5).

For severity classification, the overall accuracy is 94.5%. From the classification results of subclasses, the model shows low sensitivity (88.2%) for identifying severe cases, but good specificity (100.0%). For sagittal alignment, the accuracy, sensitivity, and specificity of distinguishing normal or abnormal PTK were 98.6%, 99.3%, and 87.5%, respectively. MTK was 93.8%, 95.8%, 81.5%, TSA was 91.8%, 93.6%, 86.5%.

### Automatic measurement time

In this study, the automatic measurement time involved loading image data into software or MicroDicom viewer, identifying the upper and lower end vertebra, drawing the upper and lower endlines, and obtaining measurements of CA at different locations. We only compared the differences in automatic measurement time among the patient groups, as in some images of the healthy group, there was no scoliosis and it was difficult to measure CA. We aimed to observe the automatic measurement efficiency of AI. The average model time

was 9.1 s ( $\pm 1.4$  s), which was significantly lower than the manual time of 185.1 s ( $\pm 37.7$  s), and the t-test showed that the difference was statistically significant ( $P < 0.001$ ) (Fig. 6).

### Discussion

In this study, we developed a deep learning model based on biplane radiographs. It can automatically measure coronal and sagittal alignment parameters. We tested the validity of the model, including CA measurement values, severity classification, and evaluation of sagittal anomalies. The results indicate that our model has a good generalization ability and robustness, and can accurately detect keypoint in the coronal and sagittal radiographs.

CA is an important parameter for quantifying the severity of scoliosis. Compared with the GS, our model showed that the MAD of total CAs in the coronal plane was 2.15°, and the ICC was 0.985. It also achieved excellent results in sagittal parameters measurement, with a MAD of 2.72° and ICC of 0.927. Recently, methods based on vertebral segmentation and landmark detection have been widely used in scoliosis and have achieved good accuracy. Previous studies reported the mean difference as 2–8° [9, 11, 21–23]. Some studies have reported that the error in automatically measuring MTK is about 7° [12], but there is currently no measurement for PTK and TSA. Our automatic measurement errors on PTK, MTK, and TSA were 2.86°, 3.20°, and 2.11°, respectively. We excluded images such as clothing or shoulder joint obstruction, which may be the reason for

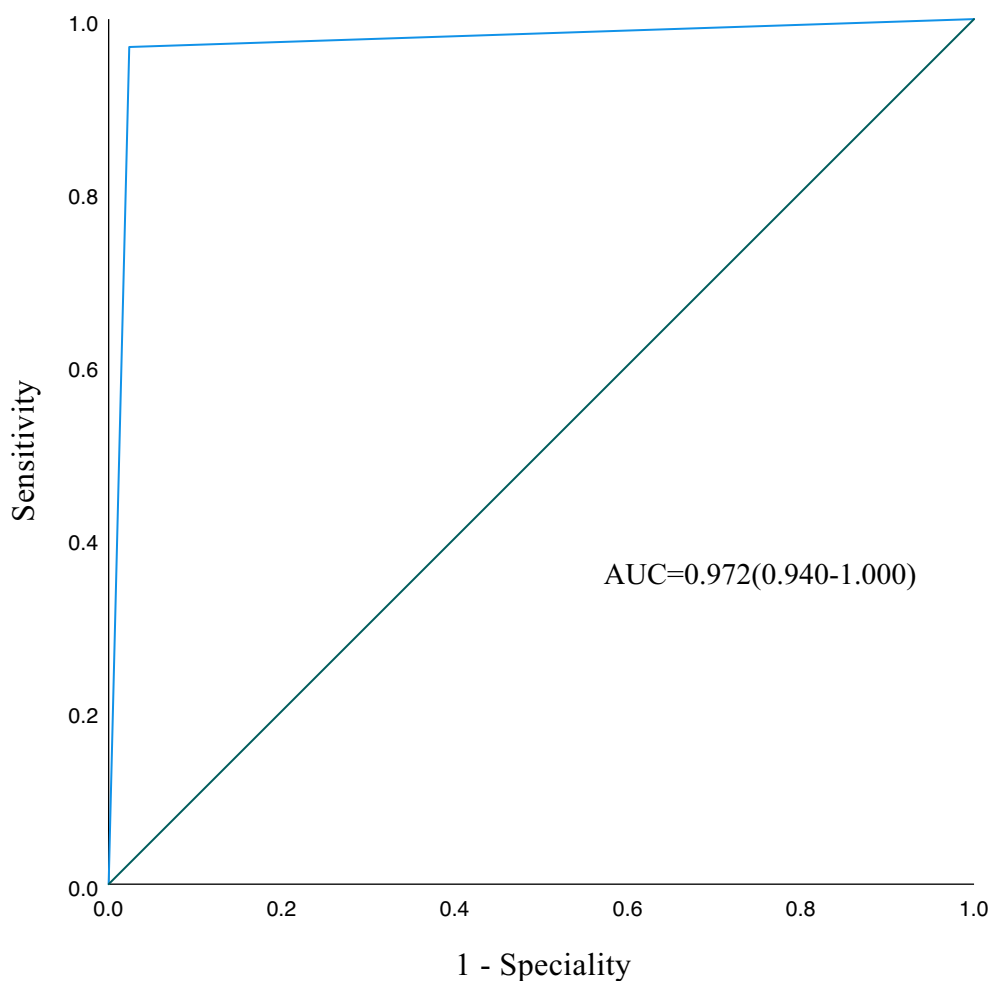


**Fig. 4** Model diagnostic performance. The ROC curve demonstrated the excellent diagnostic performance of AI

the improved accuracy. However, the unclear vertebral features remain one of the challenges faced by lateral automated measurement. In addition, the results of simple linear regression indicated a strong correlation between our model and the GS ( $r^2 \geq 0.686$ ,  $p < 0.001$ ). The Bland-Altman plots show that the mean difference of the measured values in the coronal and sagittal planes is  $0.4803^\circ$  and  $1.224^\circ$ , respectively. The above results indicated that our model has better reliability and validity, which may be related to using ResNet34 as the network backbone. It has an excellent performance in keypoint detection, can accurately identify vertebral corners, and has excellent image generalization ability.

However, the radiograph may be non-standard when the spine rotates or tilts during the image capture process. The non-standard AP or lateral radiograph can indeed lead to errors in measurement of spine parameters [24, 25]. A solution to this problem is that the AI model should assess the quality of spine

radiographs before measuring them to eliminate the potential errors. Some parameters should be designed to evaluate the rotation and tilt of the lateral radiograph [26]. Another solution is to correct non-standard radiograph to standard radiograph [27]. However, this correction algorithm needs a powerful calculation engine and geometric theory supports. But there has been no breakthrough in the correction algorithm until now. However, this correction algorithm is promising in the future. The current AI model can only achieve intelligent radiographic measurements and cannot evaluate whether the radiographs are standard or non-standard.

Accurate severity classification of AIS can help clinicians choose appropriate treatment plans [1, 23]. In this study, the model diagnosed established radiographs and classified them into normal, mild, moderate, and severe based on the CA range, with higher accuracy than previous studies [28], reaching up to 98.6%. However, the model showed low sensitivity (88.2%) in severe scoliosis.

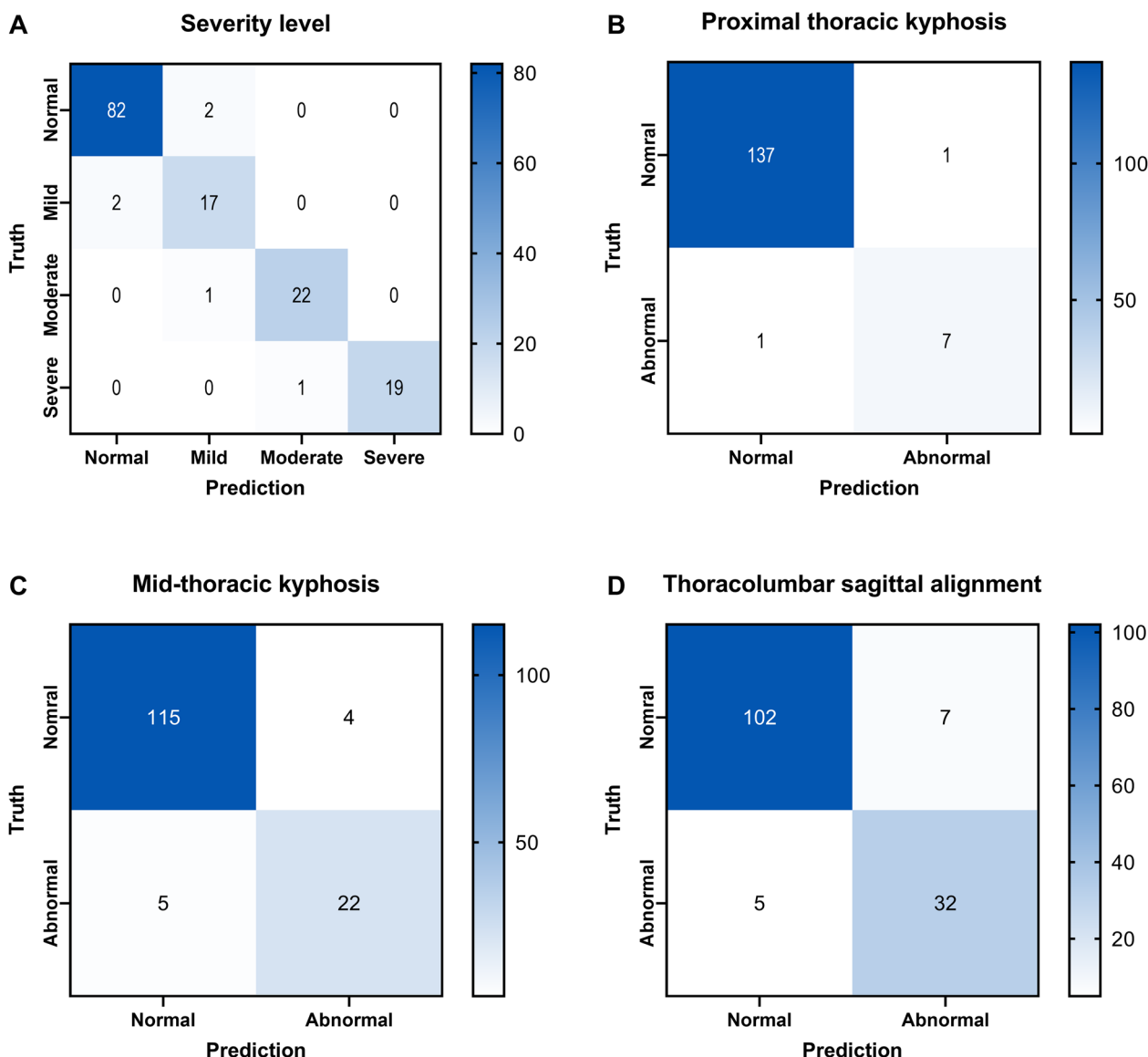


**Fig. 5** Confusion matrices for the severity classification and sagittal abnormality evaluation. **A** showed the confusion matrices for severity. **B-D** showed the confusion matrices for PTK, MTK, and TSA, respectively

In such spinal images, severe vertebral rotation, tilt [11], and unclear endplate morphology may affect vertebral corner recognition. Moreover, our model distinguished normal or abnormal sagittal parameters for the sagittal plane to assist clinicians in assessing sagittal alignment.

Most previous studies focused on the major curve CA in the coronal plane [22, 29–31] but neglected the evaluation of the alignment parameters of the minor curves and sagittal plane. In clinical practice, Each spine may have multiple curves, and the evaluation of the sagittal plane is equally important. In this study, our model calculated at least two CAs in the

coronal plane and three kyphosis angles in the sagittal plane, respectively. More importantly, it also has high accuracy in measuring the minor curve CAs, indicating that our model has certain potential in screening for scoliosis. Identifying multiple curves and determining their structural characteristics is crucial for Lenke classification [14], which contributes surgeons to making a surgery plan. Combining Bending radiographs in the future can be conducive to Lenke classification.

There are some limitations. First, the number of test sets is relatively small. This was primarily due to the limited availability of data during the initial phase of our

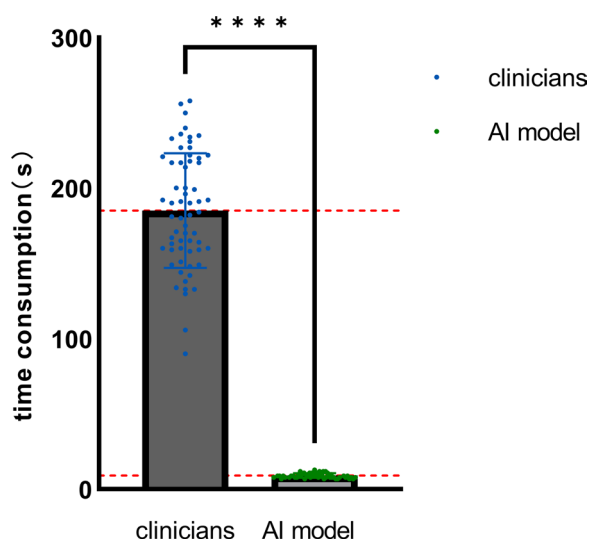


**Fig. 6** Comparison of diagnostic time between clinicians and AI model

research. Despite this constraint, we ensured that the selected test sets were representative of the variability observed in the broader population, encompassing it relevant to the study. Previous studies have effectively tested models with smaller datasets [10, 11]. Second, this study was a retrospective and was conducted at a single center. Due to differences in image size and quality, our model may experience poor performance when applied to other medical centers. Therefore, future prospective studies with multiple centers will be considered. Third, all of the radiographs were selected from AIS and normal individuals, and the image recognition performance for patients with congenital scoliosis, Marfan syndrome, and other conditions still needs to be validated. Fourth, our study did not account for the potential impact of flexible or rigid curves on the model’s automated measurements. This is because assessing spinal curve flexibility requires both anteroposterior (AP) and bending radiographs, while bending radiographs are not routinely required for AIS measurements. Further research is needed to explore this aspect in the future.

**Conclusion**

In conclusion, This deep learning model can accurately and automatically measure spinal alignment parameters with reliable results, significantly reducing diagnostic time. The model can also evaluate the severity of AIS and sagittal abnormalities. In the future, it might provide the potential to assist clinicians.

**Abbreviations**

AIS Adolescent idiopathic scoliosis  
 AP Anterior posterior

LAT	Lateral
CA	Cobb angle
EV	End vertebra
PT	Proximal thoracic
MT	Main thoracic
TL/L	Thoracolumbar/lumbarr
PTK	Proximal thoracic kyphosis
MTK	Mid-thoracic kyphosis
TSA	Thoracolumbar sagittal alignment
CNN	Convolutional neural networks
GS	Gold standard
MAD	Mean absolute difference
SD	Standard difference
ICC	Intra-class correlation coefficient

**Acknowledgements**

Not applicable.

**Author contributions**

KX wrote the first draft of the study. KX and JL participated in the analysis of the data and contributed to the interpretation of the results. SZ and YL developed algorithms and models. YL, WL, JH, and YY provided guidance on the design of the study and revised the article. WL and YY are mainly responsible for this project. All authors read and approved the final manuscript.

**Funding**

This study did not receive any funding support.

**Data availability**

No datasets were generated or analysed during the current study.

**Declarations**

**Conflict of interest**

The authors declare no competing interests.

**Ethics approval and consent to participate**

This study was performed in line with the principles of the Helsinki Declaration and was approved by the Ethical Review Board of the Xijing Hospital of the Air Force Medical University.

**Consent for publication**

Written consents for publication were obtained from all study participants.

**Author details**

<sup>1</sup>Department of Orthopedics, Xijing Hospital, Air Force Military Medical University, Xi’an 710032, China. <sup>2</sup>School of Telecommunications Engineering, Xidian University, Xi’an 710071, China.

Received: 16 October 2024 Accepted: 17 February 2025

Published online: 04 March 2025

**References**

- Weinstein SL, Dolan LA, Cheng JC, Danielsson A, Morcuende JA. Adolescent idiopathic scoliosis. *Lancet*. 2008;371(9623):1527–37.
- Rao J, Qian S, Li X, Xu Y. Single nucleotide polymorphisms of estrogen receptors are risk factors for the progression of adolescent idiopathic scoliosis: a systematic review and meta-analyses. *J Orthop Surg Res*. 2024;19(1):605.
- Altaf F, Gibson A, Dannawi Z, Noordeen H. Adolescent idiopathic scoliosis. *BMJ*. 2013;346: f2508.
- Chen X, Ye Y, Zhu Z, Zhang R, Wang W, Wu M, Lu X, Yan B, Liang Q. Association between incorrect postures and curve magnitude of adolescent idiopathic scoliosis in china. *J Orthop Surg Res*. 2024;19(1):300.

5. Fan Q, Yang J, Sha L, Yang J. Factors that influence in-brace derotation effects in patients with adolescent idiopathic scoliosis: a study based on EOS imaging system. *J Orthop Surg Res.* 2024;19(1):293.
6. Prestigiacomo FG, Hulsbosch MHHM, Bruls VEJ, Nieuwenhuis JJ. Intra- and inter-observer reliability of Cobb angle measurements in patients with adolescent idiopathic scoliosis. *Spine Deform.* 2022;10(1):79–86.
7. Kuklo TR, Potter BK, Polly DW, O'Brien MF, Schroeder TM, Lenke LG. Reliability analysis for manual adolescent idiopathic scoliosis measurements. *Spine.* 2005;30(4):444–54.
8. Liu J, Zhang H, Dong P, Su D, Bai Z, Ma Y, Miao Q, Yang S, Wang S, Yang X. Intelligent measurement of adolescent idiopathic scoliosis x-ray coronal imaging parameters based on VB-Net neural network: a retrospective analysis of 2092 cases. *J Orthop Surg Res.* 2025;20(1):9.
9. Wu C, Meng G, Lian J, Xu J, Gao M, Huang C, Zhang S, Zhang Y, Yu Y, Wang H, et al. A multi-stage ensemble network system to diagnose adolescent idiopathic scoliosis. *Eur Radiol.* 2022;32(9):5880–9.
10. Zhao Y, Zhang J, Li H, Gu X, Li Z, Zhang S. Automatic Cobb angle measurement method based on vertebra segmentation by deep learning. *Med Biol Eng Compu.* 2022;60(8):2257–69.
11. Sun Y, Xing Y, Zhao Z, Meng X, Xu G, Hai Y. Comparison of manual versus automated measurement of Cobb angle in idiopathic scoliosis based on a deep learning keypoint detection technology. *Eur Spine J.* 2022;31(8):1969–78.
12. Grover P, Siebenwirth J, Caspari C, Drange S, Dreischarf M, Le Huec J-C, Putzier M, Franke J. Can artificial intelligence support or even replace physicians in measuring sagittal balance? A validation study on preoperative and postoperative full spine images of 170 patients. *Eur Spine J.* 2022;31(8):1943–51.
13. Gstoettner M, Sekyra K, Walochnik N, Winter P, Wachter R, Bach CM. Inter- and intraobserver reliability assessment of the Cobb angle: manual versus digital measurement tools. *Eur Spine J.* 2007;16(10):1587–92.
14. Lenke LG, Betz RR, Harms J, Bridwell KH, Clements DH, Lowe TG, Blanke K. Adolescent idiopathic scoliosis: a new classification to determine extent of spinal arthrodesis. *J Bone Joint Surg Amer.* 2001;83(8):1169–81.
15. O'Brien MF, Kuklo TR, Blanke KM, Lenke LG. Radiographic measurement manual. Spinal deformity study group (SDSG). Medtronic Sofamor Danek; 2008.
16. Zhu Y, Zhang X, Fan Y, Zhou Z, Gu G, Wang C, Feng C, Chen J, He S, Ni H. Sagittal alignment of the cervical spine: radiographic analysis of 111 asymptomatic adolescents, a retrospective observational study. *BMC Musculoskelet Disord.* 2022;23(1):840.
17. He K, Zhang X, Ren S, Sun J. Deep residual learning for image recognition. In: 2016 IEEE conference on computer vision and pattern recognition (CVPR) 2016: 770–778.
18. Ronneberger O, Fischer P, Brox T. U-Net: convolutional networks for biomedical image segmentation. In: Navab N, Hornegger J, Wells WM, Frangi AF, editors. *Medical Image Computing and Computer-Assisted Intervention – MICCAI 2015*. Cham: Springer International Publishing; 2015.
19. Yi J, Wu P, Huang Q, Qu H, Metaxas DN. Vertebra-focused landmark detection for scoliosis assessment. 2020 IEEE 17th international symposium on biomedical imaging (ISBI) 2020:736–740.
20. Koo TK, Li MY. A guideline of selecting and reporting intraclass correlation coefficients for reliability research. *J Chiropr Med.* 2016;15(2):155–63.
21. Ha AY, Do BH, Bartret AL, Fang CX, Hsiao A, Lutz AM, Banerjee I, Riley GM, Rubin DL, Stevens KJ, et al. Automating scoliosis measurements in radiographic studies with machine learning: comparing artificial intelligence and clinical reports. *J Digit Imag.* 2022;35(3):524–33.
22. Liu J, Yuan C, Sun X, Sun L, Dong H, Peng Y. The measurement of Cobb angle based on spine X-ray images using multi-scale convolutional neural network. *Phys Eng Sci Med.* 2021;44(3):809–21.
23. Wong JC, Reformat MZ, Parent EC, Stampe KP, Southon Hryniuk SC, Lou EH. Validation of an artificial intelligence-based method to automate Cobb angle measurement on spinal radiographs of children with adolescent idiopathic scoliosis. *Eur J Phys Rehabil Med.* 2023;59(4):535–42.
24. Janusz P, Tyrakowski M, Monsef JB, Siemionow K. Influence of lower limbs discrepancy and pelvic coronal rotation on pelvic incidence, pelvic tilt and sacral slope. *Eur Spine J.* 2016;25(11):3622–9.
25. Hayden AM, Hayes AM, Brechbuhler JL, Israel H, Place HM. The effect of pelvic motion on spinopelvic parameters. *Spine J.* 2018;18(1):173–8.
26. Sha J, Huang L, Chen Y, Lin J, Fan Z, Li Y, Yan Y. A novel approach for screening standard anteroposterior pelvic radiographs in children. *Eur J Pediatr.* 2023;182(11):4983–91.
27. Li C, Yan Y, Xu H, Cao H, Zhang J, Sha J, Fan Z, Huang L. Comparison of transfer learning models in pelvic tilt and rotation measurement in pediatric anteroposterior pelvic radiographs. *J Digit Imag.* 2022;35(6):1506–13.
28. Zeruali M, Parpaleix A, Benbakoura M, Rigault C, Champsaur P, Guenoun D. Automatic deep learning-based assessment of spinopelvic coronal and sagittal alignment. *Diagn Interv Imag.* 2023;104(7–8):343–50.
29. Caesarendra W, Rahmaniar W, Mathew J, Thien A. Automated Cobb angle measurement for adolescent idiopathic scoliosis using convolutional neural network. *Diagnostics.* 2022;12(2):396.
30. Wu H, Bailey C, Rasoulinejad P, Li S. Automated comprehensive Adolescent Idiopathic Scoliosis assessment using MVC-Net. *Med Image Anal.* 2018;48:1–11.
31. Pan Y, Chen Q, Chen T, Wang H, Zhu X, Fang Z, Lu Y. Evaluation of a computer-aided method for measuring the Cobb angle on chest X-rays. *Eur Spine J.* 2019;28(12):3035–43.

### Publisher's Note

Springer Nature remains neutral with regard to jurisdictional claims in published maps and institutional affiliations.